

Chemical Probes Reveal Sirt2's New Function as a Robust "Eraser" of Lysine Lipoylation

Yusheng Xie,^{1,2†} Lanfang Chen,^{3†} Rui Wang,^{4†} Jigang Wang,⁵ Jingyu Li,⁴ Wei Xu,⁴ Yingxue Li,⁴ Shao Q. Yao,⁶ Liang Zhang,^{2,4*} Quan Hao,^{3*} and Hongyan Sun^{1,2*}

¹Department of Chemistry and COSDAF (Centre of Super-Diamond and Advanced Films), City University of Hong Kong, 83 Tat Chee Avenue, Kowloon, Hong Kong, China

²Key Laboratory of Biochip Technology, Biotech and Health Centre, Shenzhen Research Institute of City University of Hong Kong, Shenzhen, 518057, China

³School of Biomedical Sciences, University of Hong Kong, Hong Kong, China

⁴Department of Biomedical Science, College of Veterinary Medicine and Life Sciences, City University of Hong Kong, 83 Tat Chee Avenue, Kowloon, Hong Kong, China

⁵Department of Pharmacology, National University of Singapore, Singapore

⁶Department of Chemistry, National University of Singapore, Singapore

KEYWORDS: *Chemical probes, Lysine lipoylation, Sirtuins, Photo-crosslinking, Proteomic profiling*

ABSTRACT: Lysine lipoylation, a highly conserved lysine PTM, plays a critical role in regulating cell metabolism. The catalytic activity of a number of vital metabolic proteins, such as pyruvate dehydrogenase (PDH), depends on lysine lipoylation. Despite its important roles, the detailed biological regulatory mechanism of lysine lipoylation remains largely unexplored. Herein we designed a powerful affinity-based probe **KPlip** to interrogate the interactions of lipoylated peptide/proteins under native cellular environment. Large-scale chemical proteomics analysis revealed a number of binding proteins of **KPlip**, including Sirt2, an NAD⁺-dependent protein deacylase. To explore the potential activity of Sirt2 toward lysine lipoylation, we designed a single-step fluorogenic probe **KTlip**, which reports delipoylation activity in a continuous manner. The results showed that Sirt2 led to significant delipoylation of **KTlip**, displaying up to 60-fold fluorescence increase in the assay. Further kinetic experiments with different peptide substrates revealed that Sirt2 can catalyze the delipoylation of peptide (DLAT-PDH, K259) with a remarkable catalytic efficiency (k_{cat}/K_m) of $3.26 \times 10^3 \text{ s}^{-1}\text{M}^{-1}$. The activity is about 400-fold higher than that of Sirt4, the only mammalian enzyme with known delipoylation activity. Furthermore, overexpression and silencing experiments demonstrated that Sirt2 regulates the lipoylation level and the activity of endogenous PDH, thus unequivocally confirming that PDH is a genuine physiological substrate of Sirt2. Using our chemical probes, we have successfully established the relationship between Sirt2 and lysine lipoylation in living cells for the first time. We envision that such chemical probes will serve as useful tools for delineating the roles of lysine lipoylation in biology and diseases.

Posttranslational modifications (PTMs) of lysine residues are highly prevalent in living organisms and play important roles in regulating diverse biological processes such as gene transcription, DNA repair, chromatin structure modulation and metabolism.¹ Notable examples of lysine PTMs include methylation, acetylation, lipidation, ubiquitination, sumoylation, and others.^{1b} Recently the discovery of numerous new lysine acylations, such as succinylation (Ksucc), crontonylation (Kcr), 2-hydroxyisobutyrylation (Khib), β -hydroxybutyrylation (Kbhb), has further expanded the landscapes of lysine PTMs.² Deciphering the regulatory mechanisms of these new lysine PTMs is important to further elucidate their biological functions. Research in this field has therefore seen tremendous development and attracted increasing attention in recent years.

Lysine lipoylation (Klip) is a highly conserved lysine PTM found in bacteria, virus and mammals.³ It plays a critical role in regulating cell metabolism. Klip is reported to occur on several essential metabolic multimeric complexes, including the branched-chain α -ketoacid dehydrogenase (BCKDH), the α -ketoglutarate dehydrogenase (KDH) complex, the pyruvate dehydrogenase (PDH) complex and the glycine cleavage complex (GCV).^{3b,c} Klip is required as an essential cofactor for maintaining the activity of these enzyme complexes.⁴ Malfunction of these metabolic complexes, on the other hand, can lead to numerous diseases.^{3e,5} For instance, dysregulation of PDH activity has been linked to many diseases including metabolic disorders, cancer, Alzheimer's disease and viral infection.⁶ Notwithstanding

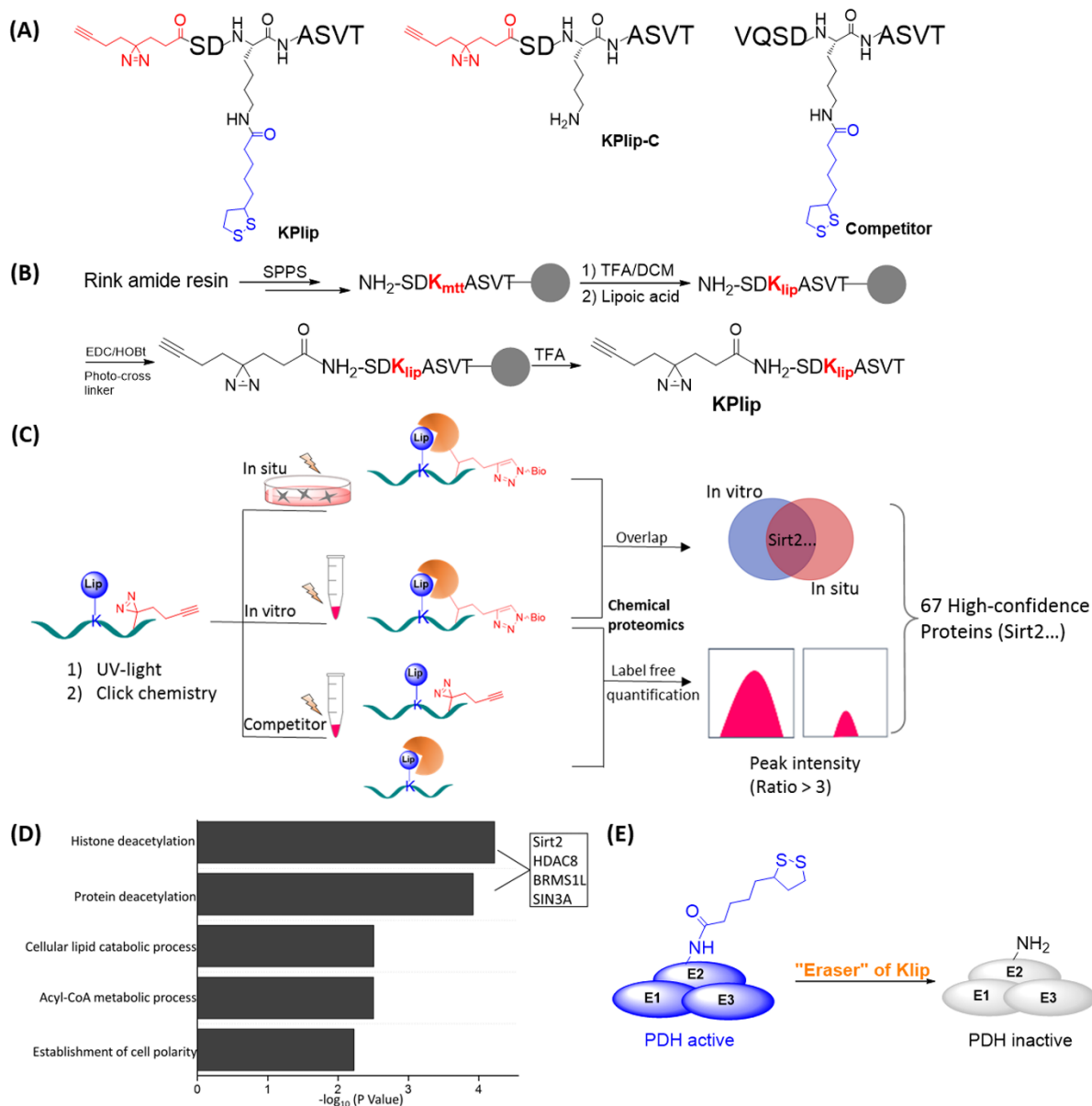


Figure 1. (A) Chemical structures of probe **Klip**, its negative control probe **Klip-C** and Competitor. (B) Synthetic route of probe **Klip** via solid phase peptide synthesis approach (SPPS). (C) Overall scheme of the chemical proteomic experiments to identify high confidence binding proteins of **Klip**. A series of chemical proteomic experiments were performed, including **Klip**/**Klip-C** with live cells/cellular lysates and competition experiments. (D) Gene ontology analysis of the 67 proteins identified by **Klip** reveals their association with a number of biological processes, e.g. protein deacetylation process. The names of the four proteins belonging to the functional cluster of "histone/protein deacetylation" are shown. (E) Scheme showing PDH activity is regulated by delipoylation.

the important roles of lysine lipoylation in biology, its regulatory mechanisms, in particular the enzymes that catalyze the removal ("erasers") of this PTM, are still poorly understood. In 2013, Denu et al. screened the *in vitro* deacylation activity of sirtuins against histone peptides with various acyl modifications including lipoylation.⁷ However, there remains a lack of knowledge of lysine lipoylation regulation, such as detailed enzymatic activity and *in vivo* substrate specificity. Elucidating the regulatory mechanism of lysine lipoylation will help understand its roles in biology and various diseases.

In a recent seminal work, Cristea et al. discovered that Sirt4 could interact with PDH complex using immunoenrichment methods.^{3c} The study revealed that Sirt4 is the first mammalian enzyme that can modulate PDH activity through delipoylation in living cells. However, it was noted that the delipoylation activity of Sirt4 *in vitro* was rather weak, especially when compared with the deacetylation activity of sirtuins.^{3c, d, 7-8} This raises an intriguing question--whether there are other enzymes that can erase Klip more efficiently in native cellular environment.

To address this question, we endeavored to develop robust chemical tools to aid in understanding the biological functions of lysine lipoylation. Specifically in this study, we have successfully developed the first affinity-based probe **KPlip** capable of interrogating the lipoylated peptide/protein interactions under native cellular environments. This chemical probe allows us to identify potential regulators of lysine lipoylation, thus uncovering new biology related to lipoylation. Furthermore, we have developed a fluorogenic probe **KTlip** to detect delipoylation activity in a continuous manner. The probe enables us to quickly and reliably examine whether a given protein possesses delipoylation activity.

Results

Chemical Proteomic profiling using probe KPlip. Profiling the interaction between an enzyme and its substrate is challenging, as their interactions are usually weak, transient and dynamic.⁹ Affinity-based-probes (A/BPs) provide a powerful tool to overcome those hindrances by utilizing photo-cross-linking to convert transient protein-ligand interactions into covalent chemical linkages.¹⁰ Chemical proteomics using A/BPs coupled to mass spectrometry is a robust strategy that facilitates elucidation of complex molecular mechanisms by studying protein-ligand interactions within signaling networks.^{10b, c} To identify potential regulators of Klip, we first designed and synthesized an A/BP, **KPlip** (Fig. 1A), on the basis of a peptide sequence derived from BCKDH protein (K105, QSDK_{lip}ASVT). In the probe design, the N-terminal Gln residue was replaced by a photo-crosslinker. To synthesize **KPlip**, the peptide was firstly assembled by standard Fmoc solid phase peptide synthesis (SPPS) method. The Mtt group in the peptide was then deprotected to allow the installation of a lipoyl group. Subsequently a photo-cross-linker with diazirine was introduced to the peptide (Fig. 1B). **KPlip** was further purified by HPLC and characterized by LC-MS. For comparison study, we also synthesized a control probe **KPlip-C** without the lipoyl moiety (Fig. 1A).

With the two probes in hand, we next performed chemical proteomics experiments (Fig. 1C), aiming to pull down potential interacting proteins of **KPlip** in cellular environment. To minimize “false hits” produced by non-specific protein binding, probe **KPlip-C** was used in parallel as a negative control. Briefly, probes (10 μ M) were incubated with live HEK 293 cells or lysates for 2 h. Following ultraviolet (UV) irradiation, the **KPlip/ KPlip-C** labeled proteomes were clicked with biotin-azide, enriched by affinity purification, resolved by SDS-PAGE, and finally analyzed by LC-MS/MS. Upon removal of non-specific binding proteins identified from the control probe **KPlip-C**, only the proteins which were positively identified in both live-cell and lysate experiments were chosen as potential targets. This led to a probe-selectivity list of 419 protein candidates (Supplementary Data 2).

Next, we performed a series of competition experiments to further identify the high-specificity binders of **KPlip** (Fig. 1C). HEK 293 cell lysates were preincubated with DMSO or a lipoylated peptide competitor (VQSDK_{lip}ASVT, Fig. 1A) at 100 μ M. Subsequently the lysates were labeled with probe **KPlip** (10 μ M) by UV irradiation. The probe-labeled proteomes were then conjugated with biotin-azide, enriched by streptavidin beads, resolved by SDS-PAGE, digested with

trypsin, and finally analyzed by label-free LC-MS/MS quantitation. High-specificity binders of **KPlip** were defined as those showing substantial signal decrease (≥ 3 -fold) in the presence of the competitor. This led to a total of 588 proteins identified (Supplementary Data 2). We compared the proteins identified in both the probe-selectivity and competition experiments, leading to a high-confidence list of 67 **KPlip**-binding proteins. (Supplementary Data 2).

We then performed the Gene Ontology (GO) analysis of the high-confidence **KPlip**-binding proteins. It revealed that a variety of biological processes, such as cellular lipid catabolic process and acyl-CoA metabolic process (Supplementary Data 3), were significantly enriched. Specifically, “histone/protein deacetylation” list caught our attention, because they may include proteins that regulate Klip modification. These proteins are summarized in Figure 1D. It is interesting to note that Sirt2, a member of the sirtuin family of NAD⁺-dependent HDAC,¹¹ is among the “histone/protein deacetylation” list. The sirtuin proteins have been reported to mediate the hydrolysis of various acyl groups of lysine, including Ksucc, Kmal, and others.¹² The fact that Sirt2 is among the Klip-interacting proteomes prompted us to investigate its role in regulating lysine lipoylation. It was also noted that Sirt4 was not identified in our protein list. A plausible reason is the instability and the low abundance of Sirt4 in human proteome (Paxdb, www.paxdb.org)

In-gel labeling of KPlip. To further validate the interaction between Klip and Sirt2, we first examined the labeling efficiency of **KPlip** with recombinant Sirt2. The enzyme was first incubated with either **KPlip** or a negative control probe **KPlip-C** followed by 15 min of UV irradiation. Upon click chemistry with rhodamine azide (Rh-N₃), the reaction mixtures were resolved by SDS-PAGE and analyzed by in-gel fluorescence scanning. The results (Fig. 2A) showed that Sirt2 was labeled by **KPlip** efficiently, whereas no labeling was observed in the control probe **KPlip-C**, suggesting that Sirt2 interacts with the probe **KPlip** by specifically recognizing the Klip moiety. Time-dependent experiments showed that 2-min UV irradiation resulted in intense labeling (Fig. 2B). The fluorescence intensity of the labeled Sirt2 band increased when the concentrations of the probe increased, demonstrating that probe **KPlip** labeled the target protein in a concentration-dependent manner (Fig. 2C). Further selectivity study revealed that probe **KPlip** labeled Sirt2 much more strongly than other sirtuins did (Fig. 2D), suggesting that Sirt2 recognizes lipoylated lysine more preferentially than other sirtuins do. To examine whether lipoic acid of **KPlip** forms disulfide bond with cysteine residues in Sirt2, excessive reducing reagent TCEP was added to the solution containing Sirt2 and **KPlip** prior to UV irradiation. No diminished effect of Sirt2 labeling was observed (Fig. 2E, Fig. S26C & D), suggesting the labeling of Sirt2 by probe **KPlip** was not redox-based. Moreover, the labeling of Sirt2 can be inhibited by a lipoylated peptide competitor (VQSDK_{lip}ASVT, Fig. 1A) verifying that the interaction between Sirt2 and lipoylated peptide is selective and direct (Fig. 2F).

Pull down validation of KPlip. We first performed live cell labeling with **KPlip**. As shown in Fig. 2G, several major bands were fluorescently labeled. Probe **KPlip-C** and DMSO control showed very faint or no labeling, indicating that

probe **KPlip** recognized these proteins in specific manner. We next validate the physiological interaction of Klip and Sirt2 using pull down experiments. 10 μM **KPlip** was used to incubate with live HEK 293 cells for 2 h. The treated cells were subsequently UV-irradiated and subjected to click reaction with biotin-azide (**Bio-N₃**). The cells were then lysed

and subjected to enrichment with streptavidin beads. The enriched proteins were finally analyzed by western blotting with anti-Sirt2. As shown in Fig. 2G, Sirt2 was successfully pulled

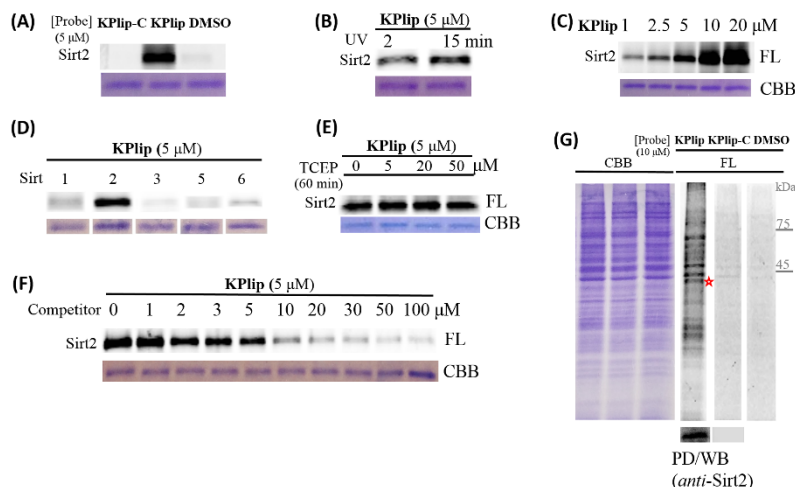


Figure 2. (A) Recombinant Sirt2 was labeled by probe **KPlip** but not by control probe **KPlip-C**. (B) Time-dependent UV irradiation labelling of **KPlip** with recombinant Sirt2. (C) Concentration-dependent labeling of **KPlip** with recombinant Sirt2 after 15 min of UV irradiation. (D) Labeling profiles of **KPlip** with recombinant Sirt1, Sirt2, Sirt3, Sirt5 and Sirt6. (E) Labeling of Sirt2 by **KPlip** was not affected by reducing reagent TCEP. (F) Labeling of Sirt2 by **KPlip** was inhibited in a dose-dependent manner by a lipoylated peptide competitor. A-F: enzyme loading: 0.33 $\mu\text{g}/\text{lane}$. (G) In-gel labelling of live HEK293 cells with probe **KPlip**. The potential Sirt2 band was labeled with an asterisk. Protein loading: 16 $\mu\text{g}/\text{lane}$. The corresponding pull-down (PD)/ Western blot (WB) results with *anti*-Sirt2 were shown at the bottom. Results show that endogenous Sirt2 can be pulled down with probe **KPlip** but not probe **KPlip-C**.

down by **KPlip**. In contrast, Sirt2 was not observed in the absence of probe or with the control probe (**KPlip-C**) (Fig. 2G). These results unambiguously proved that endogenous Sirt2 can be pulled down by lipoylated peptides under native cellular environment. In addition, we also performed pull-down assay to validate the binding of HDAC8/BRMS1L to Klip. The results show that both proteins can be effectively pulled down by **KPlip** (Fig. S28). This is consistent with the LC-MS/MS results. These experiments indicate that **KPlip** is a reliable tool for chemical proteomics to dissect proteins interacting with lipoylated lysine.

Delipoylation study with probe **KTlip.** After confirming the interactions of Sirt2 and lipoylated peptide in cellular context, we next investigate whether Sirt2 is capable of removing lipoyl modification. To this end, we set out to develop fluorescent probes to detect delipoylation activity. Compared with mass spectrometry,¹³ radioisotopes,¹⁴ specific antibodies and HPLC,¹⁵ fluorescent probes possess prominent advantages in detecting enzyme activity, such as high sensitivity and simple procedure.¹⁶ Until now, no single-step fluorescent probe has been developed to report delipoylation activity. In fact, it is difficult to design single-step fluorescent probes for detecting deacetylation activity because the aliphatic amide structure in Kacyl group does not allow conjugation to a fluorophore.^{16d} We have previously designed fluorescent probes to detect deacetylation activity of HDACs through intramolecular reaction strategy.^{9b} We reasoned that this approach would be useful for

reporting delipoylation activity, but at the same time it may face the problem of substrate recognition of enzyme because the size of Klip is larger than that of Kac. In this study, we designed a fluorogenic probe **KTlip** for profiling delipoylation activity in vitro. As shown in Fig. 3A, the probe consists of a recognition group, Klip and an *O*-NBD moiety. We hypothesize that when enzymes hydrolyze the lipoyl group, the released amine will attack the *O*-NBD, yielding *N*-NBD and turn on the fluorescence. (Fig. 3A, Scheme. S9). Such a probe can report the delipoylation activity of enzymes continuously and reliably.

We first synthesized probe **KTlip** following the synthetic route (Scheme. S2). We then examined the capacity of HDACs to recognize and remove the lipoyl group of **KTlip** by fluorimeter assay. Briefly, **KTlip** was incubated with various HDACs at 37 $^{\circ}\text{C}$ in HEPES buffer (*pH* 8.0). The fluorescence of the enzymatic reactions was then measured accordingly. As shown in Fig. 3C, Sirt2 showed the strongest fluorescence increment, with 60-fold fluorescence increase. Sirt1 showed much lower fluorescence signal, whereas Sirt3, Sirt5, Sirt6 and HDAC8 did not show noticeable fluorescence increase. The control group without cofactor NAD^{+} displayed negligible fluorescence, indicating the reaction occurred through enzymatic catalysis. Further HPLC and MS analysis confirmed that the molecular weight of the newly generated peak corresponded to the expected tandem delipoylated/exchanged product (Fig. S14 A & B). It was noted that no delipoylated product was observed under

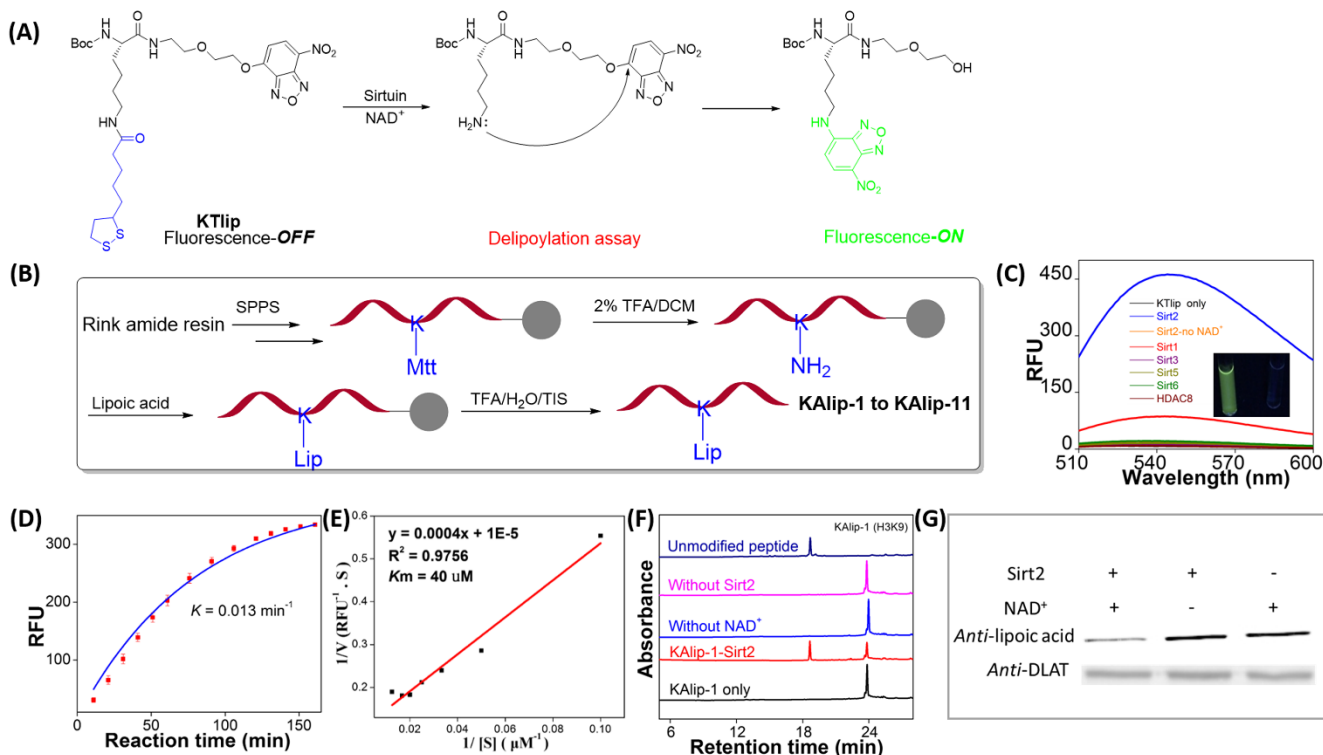


Figure 3. (A) Schematic illustration of the fluorescence "turn-on" mechanism of probe **KTip** through a delipoylation reaction. (B) Synthetic scheme of lipoylated peptides **KAlip-1** to **KAlip-11** by SPPS. (C) Fluorescence measurement of **KTip** (10 μM) with sirtuins and HDAC8 (40 ng/μL) (λ_{ex} = 480 nm). The enzymatic reaction product displayed green fluorescence (inset). (D) Time-dependent fluorescence measurement of **KTip** (10 μM) with Sirt2 (40 ng/μL), λ_{ex} = 480 nm, λ_{em} = 545 nm. (E) Lineweaver-Burk plot analysis of **KTip** with Sirt2. (F) HPLC analysis of the enzymatic reaction of representative peptide **KAlip-1** (40 μM) with Sirt2 (80 ng/μL). The reaction was monitored at 280 nm. The retention time of the newly generated peak matched well with that of the peptide without lipoyl group. (G) Sirt2 delipoylated recombinant DLAT protein in the presence of cofactor NAD⁺.

Table 1. Delipoylation study of Sirt2 with various lipoylated peptides.

| Peptide | Protein/Lysine residue | Peptide sequence | Delipoylation product ^a | k_{cat} (S ⁻¹) | K_m (μM) | k_{cat}/K_m (S ⁻¹ M ⁻¹) |
|-----------------|----------------------------------------|---------------------|------------------------------------|------------------------------|------------|--------------------------------------------------|
| KAlip-1 | Histone, H3K9 | KQTARK(lip)STGGWW | 59% | 0.01 ± 0.0003 | 9.7 ± 0.2 | 1.06 × 10 ³ |
| KAlip-2 | Dps, K10 | VKSK(lip)ATNLWW | 97% | ~ | ~ | ~ |
| KAlip-3 | Pyruvate kinase, K105 | SDPIIK(lip)GSGTWW | 98% | ~ | ~ | ~ |
| KAlip-4 | GDH, K503 | SGASEK(lip)DIVHSGWW | 100% | ~ | ~ | ~ |
| KAlip-5 | PDH, E2, K259 | EIETDK(lip)ATIGWW | 100% | 0.061 ± 0.002 | 18.9 ± 0.6 | 3.26 × 10 ³ |
| KAlip-6 | PDH, E3, K97 | EIETDK(lip)AVVTWW | 100% | ~ | ~ | ~ |
| KAlip-7 | KDH, E2, K110 | EIETDK(lip)TSVQWW | 65% | ~ | ~ | ~ |
| KAlip-8 | BCKDH, E2, K105 | VQSDK(lip)ASVTWW | 100% | 0.045 ± 0.0002 | 26.2 ± 3.3 | 1.72 × 10 ³ |
| KAlip-9 | TNF-α, K20 | EALPKK(lip)TGGPWW | 100% | ~ | ~ | ~ |
| KAlip-10 | Glycine cleavage system, K107, | ALESVK(lip)AASEWW | 71% | ~ | ~ | ~ |
| KAlip-11 | Biotin carboxyl carrier protein, K122, | VEAMK(lip)LMNEWW | 94% | 0.023 ± 0.0002 | 13.5 ± 1.4 | 1.67 × 10 ³ |

^a HPLC yield of delipoylated product was monitored at 280 nm after 40 mins.; ~ indicates data was undetermined.

the enzymatic reaction condition for HDAC8 (Fig. S16). After enzymatic reaction with Sirt2, a shift of peak absorption from 380 nm to 480 nm was clearly observed. (Fig. S14C). Through detailed kinetic study, the first order rate constant of the reaction was determined to be 0.013 min^{-1} (Fig. 3D). The K_m value of **KTlip** obtained from the fluorescent method matched well with that from the traditional HPLC method (Fig. 3E & Fig. S15), underscoring that probe **KTlip** can serve as a useful tool for detecting enzymatic delipoylation activity. These data revealed that Sirt2 displays robust activity to remove lipoyl group in vitro.

Delipoylation study with various lipoylated peptides. Encouraged by the above results, we next investigated whether sirtuins exhibit substrate specificity in recognizing different peptide sequences.¹⁷ To this end, we designed and synthesized a total of 11 lipoylated peptides (**KAlip-1** to **KAlip-11**, Fig. 3B). The peptide sequences were selected from reported lipoylated proteins (PDH, KDH, BCKDH and GCV) and non-lipoylated proteins (e.g. histone) (Table S1). The peptides were synthesized with standard Fmoc solid phase synthesis approach and characterized by LC-MS. The delipoylation activity was then determined by HPLC assay. Sirt2 catalyzed the removal of lipoyl group for all the peptide tested (Table 1 & Fig. 3F & S19-24). Compared with non-putative peptide, putative lipoylated peptides appear to be more efficiently hydrolyzed by Sirt2. For example, the delipoylated product of **KAlip-1** (derived from histone) after 40 min was determined to be 59%, which is less than that of putative lipoylated substrates such as **KAlip-5** and **KAlip-6** (derived from PDH). It was noted that near absolute delipoylation was observed for **KAlip-5** and **KAlip-8** within just 15 mins, signifying that Sirt2 catalyzed the removal of lipoyl group with high efficiency. Furthermore, control experiments without the addition of NAD^+ and enzyme unambiguously proved that the hydrolysis reaction is attributed to enzymatic activities rather than other environmental factors (Fig. S19-24). In addition, the newly generated peak of **KAlip-1** with Sirt2 showed the same retention time as the unmodified peptide (Fig. 3F). We also further examined HDAC8's delipoylation activity using **KAlip-5** and **KAlip-1**, no delipoylated product was observed (Fig. S17). The enzymatic delipoylation results by fluorescent probe **KTlip** and lipoylated peptide **KAlip-5** and **KAlip-1** together indicated that HDAC8 has no delipoylation activity.

To have a more detailed assessment of the enzymatic delipoylation reaction, we performed time-dependent experiments and steady-state kinetics studies of **KAlip-1**, **5**, **8** and **10** with Sirt2 (Fig. S25, Table 1 & S2). Interestingly, kinetics data (Table 1) revealed that the catalytic efficiency (k_{cat}/K_m) for delipoylation activity of Sirt2 is of the same order of magnitude as that of the deacetylation of Sirt1-2,^{12c} the desuccinylation/demalonylation of Sirt5 and the demyristoylation of Sirt6 in vitro (Table S2).^{12b, c} The catalytic efficiency of Sirt2 toward the putative lipoylated peptides (**KAlip-5**, **8**, **10**) was slightly higher than toward the non-putative H3K9 lipoyl peptide (**KAlip-1**). Strikingly, the catalytic efficiency of Sirt2 (k_{cat}/K_m) to delipoylate DLAT K259 of PDH complex (**KAlip-5**) is approximately 426-fold higher than that of Sirt4 (Table S2).^{3c} Taken together, these in vitro enzymology data demonstrated that Sirt2 is a robust delipoylating enzyme.

Sirt2 remove Klip from lipoylated DLAT protein. To test whether Sirt2 delipoylates protein substrates, recombinant DLAT protein from mammalian cells was used for a delipoylation assay. The Klip modification in DLAT was first confirmed using Western blot with a lipoic acid antibody (Fig. 3G). Subsequently DLAT was incubated with Sirt2 in the presence of cofactor NAD^+ and the lipoylation level of DLAT was examined by Western blot (Fig. 3G). Negative control with no NAD^+ or no Sirt2 were included as well. Comparing with the control groups, a substantial reduction was observed in Klip level for DLAT treated with Sirt2 in the presence of NAD^+ . These results indicated that Sirt2 has delipoylation activity towards DLAT protein.

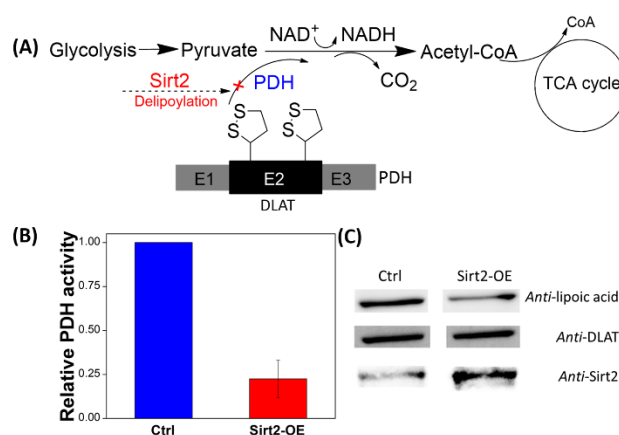


Figure 4. (A) Schematic diagram illustrating PDH catalyzes the conversion of pyruvate to acetyl-CoA, which is linked to TCA cycle. We hypothesize that PDH activity might be inhibited by Sirt2 through delipoylation. (B) Relative PDH activity comparison between HeLa-S3 cells overexpressing Sirt2 and wild-type cells. PDH activity was measured by a commercial colorimetric assay. (C) Western blot analysis of endogenous lipoylated DLAT of PDH in cells over-expressing Sirt2 versus wild-type cells. DLAT is used as loading control.

Sirt2 delipoylates PDH in living cells. Having shown that Sirt2 displayed strong delipoylation activity in vitro, we next investigated whether Sirt2 could delipoylate the physiological substrate in living cells. Lipoylated PDH is responsible for converting pyruvate into acetyl-CoA, a central metabolite that enters into TCA cycle.^{3c, 4} On the other hand, the delipoylation of PDH impairs its activity (Fig. 4A). Although the cellular localization of Sirt2 was conventionally annotated to be in cytosol/nucleus, recent literature suggests that Sirt2 could localize to mitochondria and regulate the functions of mitochondrial proteins.¹⁸ In line with this, Sirt2 was detected in the mitochondrial fraction isolated from HeLa S3 cells overexpressing Sirt2 (Fig. S29). Thus, we next endeavored to investigate whether Sirt2 can delipoylate PDH and regulate its function in living cells. To conduct the test, we overexpressed Sirt2 in HeLa S3 cells by transfecting cells with pCMV4a-Sirt2 vector. After transfection, the cells were harvested and lysed. Western blot experiments confirmed effective Sirt2 overexpression (Fig. 4C). The obtained cell lysates were then subjected to PDH activity assay. As shown in Fig 4B, PDH activity in cells overexpressing Sirt2 was significantly decreased comparing to that in wild type cells. In line with this, the lipoylation level of DLAT (E2

subunit of PDH) was decreased in cells overexpressing Sirt2, whereas the total level of DLAT remained unchanged (Fig. 4C). Furthermore, we performed siRNA knock-down experiments to examine the regulatory effect of endogenous Sirt2 on the lipoylation of PDH. Effective siRNA-mediated knock-down of Sirt2 was confirmed (Fig. S30B). Notably, Sirt2 knockdown led to an elevated lipoylation level in DLAT (Fig. S30B). Concomitantly, increased PDH activity was also observed (Fig. S30A). These results together prove that Sirt2 can effectively catalyze DLAT delipoylation and modulate PDH activity in cells.

In conclusion, we have successfully developed a panel of chemical probes to investigate the regulatory mechanism of lysine lipoylation. The developed A/BP probe **KPlip** is capable of capturing Klip-interacting proteins in both living cells and cell lysates. Notably, chemical proteomics experiments with **KPlip** identified Sirt2 as a novel binder of lipoylated substrate. **KTlip** is the first single-step fluorescent probe developed for rapid profiling of delipoylation activity. The enzymology data obtained from both **KTlip** and lipoylated peptides demonstrated the robust delipoylation ability of Sirt2 in vitro. It is noteworthy that the delipoylation activity of Sirt2 is far superior to that of Sirt4, the only identified mammalian delipoylating enzyme. Through our chemical probes, we proved the novel function of Sirt2 to remove lipoyl group with high catalytic efficiency. Furthermore, we also showed that Sirt2 could effectively catalyze DLAT delipoylation and downregulate PDH activity in cells. It is noted that a recent report showed that Sirt3 could enhance PDH activity through deacetylating the E1 subunit.¹⁹ This suggests that sirtuins might play a complex role in the dynamic regulation of PDH activity through different deacylation mechanisms. With the probes developed in this study, we envision that they will provide useful tools to further advance our understanding of lipoylation and other acylation in biology and diseases.

Materials and Methods

General Information. Sirtuins including Sirt1, Sirt2, Sirt3, Sirt5 and Sirt6, were recombinantly expressed and purified according to previous reports.^{12b, c, 17} Pyruvate Dehydrogenase E2 (DLAT) (NM_001931) human recombinant protein was from ORIGENE. Streptavidin Magnetic Beads were purchased from New England Biolabs. In-gel fluorescence scanning experiments were performed with a FLA-9000 Fujifilm scanner. Antibody of Sirt2 (D4S6J) was from Cell Signaling. Anti-bodies of DLAT (ab172617), lipoic acid (ab58724), HDAC8 (ab187139), BRMS1L (ab107171) and Hsp60 (ab128567) were from Abcam. IRDye 680RD Donkey anti-Rabbit IgG (Secondary antibody) was purchased from LI-COR Biosciences. Immobilon-FL poly(vinylidene difluoride) membrane for western blotting was purchased from Merck Millipore. Western blotting was carried out with a C600 Azure biosystem. Sirt2 siRNA (AM16708) was from Thermo Fisher Scientific. The plasmid pCMV4a-SIRT2-Flag was purchased from Addgene (Plasmid #102623).²⁰ The sequencing grade modified trypsin was purchased from Promega.

Cu(I)-Catalyzed Cycloaddition/Click Chemistry. Briefly, 20 μ M azide reagent was added to the protein samples la-

belled by **KPlip** and **KPlip-C**. Tris(2-carboxyethyl)phosphine (0.4 mM), Tris(3-hydroxypropyl)triazolylmethylamine (40 μ M) and CuSO₄ (0.4 mM) were then added. The reaction was kept at room temperature for 2 h.

Affinity Enrichment of Biotinylated Proteins. After click chemistry reaction of **KPlip** or **KPlip-C** using biotin-azide (**Bio-N₃**), chilled acetone was added to precipitate the proteins. The pellets were then washed with cold methanol and air-dried. The obtained pellets were re-dissolved in PBS buffer containing less than 0.5% sodium dodecyl sulfate (SDS) by heating and vortexing. Streptavidin magnetic beads were then added and shaken gently at room temperature for 4 h. The beads were collected by a magnet and washed with 0.1% SDS/PBS once and PBS twice. The beads were re-dissolved in 1 x SDS loading buffer and proteins were released/denatured by boiling at 95 °C for 20 min.

In-gel digestion by trypsin. The pull-down sample was separated on 12% SDS-PAGE gel and stained with Ruby protein staining method. The gel was cut into different pieces. The collected gel was washed by 100 mM ammonium bicarbonate buffer, reduced by DTT (5 mM) at 50-60 °C for 30 minutes, alkylated by iodoacetamide (25 mM) at room temperature for 45 minutes, dehydrated by 95% ethanol, digested by sequencing grade modified trypsin at 37 °C for overnight. After that, the digested solution was collected. The gel was further extracted twice using 50% acetonitrile containing 5% formic acid. The combined solution was dried by speed vacuum for LC-MS/MS analysis.

LC-MS/MS Analysis. Upon extraction from the gel and desalting, the obtained peptides were redissolved in 12 μ l of 0.1% formic acid and separated by an Easy-nLC 1200 system coupled to a Q Exactive HF (Thermo Scientific). 5 μ l of peptides were injected and separated on a reverse phase C18 column (75 μ m \times 15 cm) at a flow rate of 250 nL/min. Mobile phase A (0.1% formic acid in ultrapure water) and mobile phase B (0.1% formic acid and 80% acetonitrile in ultrapure water) were used to establish a linear gradient of 7-25% mobile phase B in 50 min. Peptides were then ionized by electrospray at 1.5 kV. The mass spectrometer was operated in positive ion mode at a resolution of 120,000, with a full MS spectrum (m/z = 350-1800) using an automatic gain control (AGC) target of 3×10^6 . Higher-energy collisional dissociation (HCD) fragmentation was conducted with the 12 most intense ions (normalized collision energy 27). MS/MS spectra were acquired with an AGC target of 1×10^5 at a resolution of 30,000. The dynamic exclusion time was set to 30 s.

Proteomics Analysis. The raw data were created by XCalibur 4.0.27 (Thermo Scientific) software and processed with Proteome Discoverer (PD) software suite 2.2 (Thermo Scientific), against *UniProt human protein database* (downloaded on 20171010) in Sequest HT node. The precursor and fragment mass tolerances were set to 10 ppm and 0.02 Da, respectively. Reversed database searches were used to evaluate false discovery rate (FDR) of protein and peptide identifications. A maximum of two missed cleavage sites of trypsin was allowed. Carbamidomethylation (C) was set as static modification, and oxidation (M) and acetyl (N-terminus) were set as variable modifications. False discovery rate

(FDR) of peptide spectrum matches (PSMs) and peptide identification were determined using the Percolator algorithm at 1% based on q-value. The abundance values of proteins were obtained via a label-free quantification method using Proteome Discoverer 2.2.²¹ Minora Feature alignment and feature mapping were applied to calculate the abundance of peptides in the MS1 scan. Lists of protein identifications and quantification are attached in Supplementary Data2.

Bioinformatic analysis. For protein functional associations and protein-protein interaction analysis, we used the web-based analytic tools. Gene ontology analysis was performed in Metascape 3.0 (<http://metascape.org>) to explore GO terms and enrichment analysis of target proteins.²² Terms with a p-value < 0.01, a minimum count of 3 and enrichment factor > 1.5 (the enrichment factor is the ratio between the observed counts and the counts expected by chance) was set as the cut-off criteria. Subsequently, we constructed the protein interaction biological networks of identified proteins based on the STRING 11.0 database (<http://www.string-db.org>) under the standard settings.²³ In addition, the network data was exported to simple tabular text. The text was used to build protein interaction networks, which were then visualized and evaluated in Cytoscape software (v.3.7.1).²⁴

In-Gel Fluorescence Scanning. After click chemistry reaction with rhodamine-azide (**Rh-N₃**), chilled acetone was added to the reaction mixtures. The reaction was then placed in -20 °C freezer for 1 h to precipitate the proteins. The pellets were washed with cold methanol and air-dried. Finally, they were re-dissolved in 1 × SDS loading buffer by heating at 95 °C for 10 min, and then resolved by SDS-PAGE. The labeled proteins were visualized using a FLA-9000 Fujifilm scanner (Ex = 532 nm).

Western Blotting. To perform Western blotting experiments, samples were first separated by SDS-PAGE and then transferred to an Immobilon-FL polyvinylidene difluoride (PVDF) membrane. The samples were blocked with 5% non-fat milk in TBST (0.1% Tween in Tris-buffered saline) at room temperature for 1.5 h. Subsequently the membrane was incubated with primary antibody (anti-sirt2/anti-lipoic acid/anti-DLAT) at 4 °C overnight. After incubation, the membrane was washed with TBST (3 × 5 min) gently at room temperature. Following that the membrane was incubated with the secondary antibody (IRDye 680RD Donkey anti-Rabbit IgG) at room temperature for another 1 h. It was then washed with TBST (3 × 5 min). Finally, the membrane was applied to fluorescence scanning.

Absorption and fluorescence study of probe KTip. The probe **KTip** was incubated with sirtuin and NAD⁺ at 37 °C in 20 mM HEPES buffer (pH 8.0) containing 150 mM NaCl, 1 mM MgCl₂ and 2.7 mM KCl. The enzymatic reaction volume was 50 μL. When the enzymatic reaction was complete, the reaction was applied for absorption and fluorescence measurement. The parameters set for absorbance measurement were: UV-Visible light, collection region: 300–550 nm. The parameters set for fluorescence measurement were: λ_{ex} = 480 nm, slit width: 5 nm, collection region: 510–600 nm.

Determination of the first-order rate constant *k*. It was calculated by fitting the fluorescence data to the following equation:

$$\text{Fluorescence intensity} = 1 - \exp(-kt).$$

Enzymatic reaction with lipoylated peptides. The lipoylated peptides **KAlip-1** to **11** was incubated with sirtuin and cofactor NAD⁺ at 37 °C in 20 mM HEPES buffer (pH 8.0) containing 150 mM NaCl, 1 mM MgCl₂ and 2.7 mM KCl. The reaction volume was set as 50 μL. At each specific reaction time point, the reaction mixtures were quenched by adding 250 μL of methanol. The reactions were vortexed and centrifuged. Supernatant was collected and then analyzed by reverse phase HPLC. The new peak generated was collected for ESI-MS or MALDI-TOF-MS analysis directly.

Kinetic study with lipoylated peptides. To determine the values of *k*_{cat} and *K*_m, Purified Sirt2 with 400 μM NAD⁺ was incubated with different concentrations of lipoylated peptide (0–120 μM) in 20 mM HEPES buffer (pH 8.0) containing 150 mM NaCl, 1 mM MgCl₂ and 2.7 mM KCl at 37 °C for 10 min (**KAlip-1** and **KAlip-10**) or 5 min (**KAlip-5** and **KAlip-8**). The reactions were quenched by adding 250 μL of methanol and then applied for HPLC analysis with a linear gradient of 5% to 85% B (acetonitrile) for 30 min. The generated delipoylated product was quantified based on the peak area monitored at 280 nm. The *K*_m and *k*_{cat} values were calculated by curve-fitting $V_{\text{initial}}/[E]$ versus $[S]$. The experiments were conducted in duplicate.

PDH activity assay. To overexpress Sirt2 in cells, pCMV4aSirt2-Flag vector were transfected into HeLa-S3 cells using Lipofectamine™ 2000 (Invitrogen). The activity of PDH was assessed by measuring absorbance at 450 nm using a microplate assay kit (Pyruvate dehydrogenase Enzyme Activity Microplate Assay, Abcam, ab109902). 1000 μg of cell protein extracts were used for PDH immunocapture in each well. The experiments were performed in duplicate.

Mitochondria isolation. The mitochondrial fraction was isolated according to the manufacturer's instructions using a mitochondria isolation kit (Thermo Fisher, Cat. No. 89874). The experiments were performed in duplicate.

ASSOCIATED CONTENT

Supporting Information. The Supporting Information is available free of charge on the ACS Publications website at DOI:

Corresponding Author

L. Zhang, liangzhang.28@cityu.edu.hk; Q. Hao, qhao@hku.hk; H. Sun, hongqysun@cityu.edu.hk

Author Contributions

[†]These authors contributed equally to this work

Notes

The authors declare no competing financial interest.

ACKNOWLEDGMENT

We are grateful for the financial support from the Research Grants Council of Hong Kong ((Nos. 11304118, 11302415 and C7037-14G)), the National Natural Science Foundation of China

(No. 21572190 and 21778044), Shenzhen Science and Technology Program (JCYJ20170413141047772, JCYJ20180507181659781), the Synthetic Biology Research & Development Programme (SBP) of National Research Foundation (SBP-P4 and SBP-P8) of Singapore.

ABBREVIATIONS

HDAC, histone deacetylase; Sirt2, Sirtuin 2; **KPlip**: activity based protein profiling probe for lipoylated lysine proteome profiling; **KTlip**: fluorescent turn-on probe for delipoylation activity profiling; **KAlip**: lipoylated peptides for delipoylation activity profiling

REFERENCES

(1) (a) Walsh, C. T.; Garneau-Tsodikova, S.; Gatto, G. J., Jr., Protein posttranslational modifications: the chemistry of proteome diversifications. *Angew. Chem., Int. Ed. Engl.* **2005**, *44*, 7342-7372; (b) Huang, H.; Lin, S.; Garcia, B. A.; Zhao, Y., Quantitative proteomic analysis of histone modifications. *Chem. Rev.* **2015**, *115*, 2376-2418; (c) Müller, M. M.; Muir, T. W., Histones: At the Crossroads of Peptide and Protein Chemistry. *Chem. Rev.* **2015**, *115*, 2296-2349; (d) Wu, Z.; Connolly, J.; Biggar, K. K., Beyond histones - the expanding roles of protein lysine methylation. *FEBS J.* **2017**, *2732*-2744.

(2) (a) Zhang, Z.; Tan, M.; Xie, Z.; Dai, L.; Chen, Y.; Zhao, Y., Identification of lysine succinylation as a new post-translational modification. *Nat. Chem. Biol.* **2010**, *7*, 58; (b) Tan, M.; Luo, H.; Lee, S.; Jin, F.; Yang, J. S.; Montellier, E.; Buchou, T.; Cheng, Z.; Rousseaux, S.; Rajagopal, N.; Lu, Z.; Ye, Z.; Zhu, Q.; Wysocka, J.; Ye, Y.; Khochbin, S.; Ren, B.; Zhao, Y., Identification of 67 histone marks and histone lysine crotonylation as a new type of histone modification. *Cell* **2011**, *146*, 1016-1028; (c) Dai, L.; Peng, C.; Montellier, E.; Lu, Z.; Chen, Y.; Ishii, H.; Debernardi, A.; Buchou, T.; Rousseaux, S.; Jin, F.; Sabari, B. R.; Deng, Z.; Allis, C. D.; Ren, B.; Khochbin, S.; Zhao, Y., Lysine 2-hydroxyisobutyrylation is a widely distributed active histone mark. *Nat. Chem. Biol.* **2014**, *10*, 365-370; (d) Xie, Z.; Zhang, D.; Chung, D.; Tang, Z.; Huang, H.; Dai, L.; Qi, S.; Li, J.; Colak, G.; Chen, Y.; Xia, C.; Peng, C.; Ruan, H.; Kirkey, M.; Wang, D.; Jensen, Lindy M.; Kwon, Oh K.; Lee, S.; Pletcher, Scott D.; Tan, M.; Lombard, David B.; White, Kevin P.; Zhao, H.; Li, J.; Roeder, Robert G.; Yang, X.; Zhao, Y., Metabolic Regulation of Gene Expression by Histone Lysine β -Hydroxybutyrylation. *Mol. Cell* **2016**, *62*, 194-206.

(3) (a) Wilkins, M. R.; Gasteiger, E.; Gooley, A. A.; Herbert, B. R.; Molloy, M. P.; Binz, P.-A.; Ou, K.; Sanchez, J.-C.; Bairoch, A.; Williams, K. L.; Hochstrasser, D. F., High-throughput mass spectrometric discovery of protein post-translational modifications. Edited by R. Huber. *J. Mol. Biol.* **1999**, *289*, 645-657; (b) Spalding, M. D.; Prigge, S. T., Lipoic Acid Metabolism in Microbial Pathogens. *Microbiol. Mol. Biol. Rev.* **2010**, *74*, 200-228; (c) Mathias, Rommel A.; Greco, Todd M.; Oberstein, A.; Budayeva, Hanna G.; Chakrabarti, R.; Rowland, Elizabeth A.; Kang, Y.; Shenk, T.; Cristea, Ileana M., Sirtuin 4 Is a Lipoamidase Regulating Pyruvate Dehydrogenase Complex Activity. *Cell* **2014**, *159*, 1615-1625; (d) Bheda, P.; Jing, H.; Wolberger, C.; Lin, H., The Substrate Specificity of Sirtuins. *Annu. Rev. Biochem.* **2016**, *85*, 405-429; (e) Rowland, E. A.; Snowden, C. K.; Cristea, I. M., Protein lipoylation: an evolutionarily conserved metabolic regulator of health and disease. *Curr. Opin. Chem. Biol.* **2018**, *42*, 76-85.

(4) Perham, R. N., Swinging Arms and Swinging Domains in Multifunctional Enzymes: Catalytic Machines for Multistep Reactions. *Annu. Rev. Biochem.* **2000**, *69*, 961-1004.

(5) Naiyanetr, P.; Butler, J. D.; Meng, L.; Pfeiff, J.; Kenny, T. P.; Guggenheim, K. G.; Reiger, R.; Lam, K.; Kurth, M. J.; Ansari, A. A.; Coppel, R. L.; López-Hoyos, M.; Gershwin, M. E.; Leung, P. S. C., Electrophile-modified lipoic derivatives of PDC-E2 elicits anti-mitochondrial antibody reactivity. *J. Autoimmun.* **2011**, *37*, 209-216.

(6) (a) Huang, G.; Cui, F.; Yu, F.; Lu, H.; Zhang, M.; Tang, H.; Peng, Z., Sirtuin-4 (SIRT4) is downregulated and associated with some clinicopathological features in gastric adenocarcinoma. *Biomed. Pharmacother.* **2015**, *72*, 135-139; (b) Miyo, M.; Yamamoto, H.; Konno, M.; Colvin, H.; Nishida, N.; Koseki, J.; Kawamoto, K.; Ogawa, H.; Hamabe, A.; Uemura, M.; Nishimura, J.; Hata, T.; Takemasa, I.; Mizushima, T.; Doki, Y.; Mori, M.; Ishii, H., Tumour-suppressive function of SIRT4 in human colorectal cancer. *Br. J. Cancer* **2015**, *113*, 492-499; (c) Pocerlich, C. B.; Butterfield, D. A., Acrolein inhibits NADH-linked mitochondrial enzyme activity: Implications for Alzheimer's disease. *Neurotoxic. Res.* **2003**, *5*, 515-519.

(7) Feldman, J. L.; Baeza, J.; Denu, J. M., Activation of the protein deacetylase SIRT6 by long-chain fatty acids and widespread deacylation by mammalian sirtuins. *J. Biol. Chem.* **2013**, *288*, 31350-31356.

(8) Pannek, M.; Simic, Z.; Fuszard, M.; Meleshin, M.; Rotili, D.; Mai, A.; Schutkowski, M.; Steegborn, C., Crystal structures of the mitochondrial deacetylase Sirtuin 4 reveal isoform-specific acyl recognition and regulation features. *Nat. Commun.* **2017**, *8*, 1513.

(9) (a) Yang, T.; Li, X. M.; Bao, X.; Fung, Y. M.; Li, X. D., Photo-lysine captures proteins that bind lysine post-translational modifications. *Nat. Chem. Biol.* **2016**, *12*, 70-72; (b) Xie, Y.; Ge, J.; Lei, H.; Peng, B.; Zhang, H.; Wang, D.; Pan, S.; Chen, G.; Chen, L.; Wang, Y.; Hao, Q.; Yao, S. Q.; Sun, H., Fluorescent Probes for Single-Step Detection and Proteomic Profiling of Histone Deacetylases. *J. Am. Chem. Soc.* **2016**, *138*, 15596-15604; (c) Rao, V. S.; Srinivas, K.; Sujini, G. N.; Kumar, G. N., Protein-protein interaction detection: methods and analysis. *Int. J. Proteomics* **2014**, *2014*, 147648.

(10) (a) Tamura, T.; Tsukiji, S.; Hamachi, I., Native FKBP12 Engineering by Ligand-Directed Tosyl Chemistry: Labeling Properties and Application to Photo-Cross-Linking of Protein Complexes in Vitro and in Living Cells. *J. Am. Chem. Soc.* **2012**, *134*, 2216-2226; (b) Li, Z.; Wang, D.; Li, L.; Pan, S.; Na, Z.; Tan, C. Y.; Yao, S. Q., "Minimalist" cyclopropene-containing photo-cross-linkers suitable for live-cell imaging and affinity-based protein labeling. *J. Am. Chem. Soc.* **2014**, *136*, 9990-9998; (c) Li, Z.; Hao, P.; Li, L.; Tan, C. Y.; Cheng, X.; Chen, G. Y.; Sze, S. K.; Shen, H. M.; Yao, S. Q., Design and synthesis of minimalist terminal alkyne-containing diazirine photo-crosslinkers and their incorporation into kinase inhibitors for cell- and tissue-based proteome profiling. *Angew. Chem., Int. Ed. Engl.* **2013**, *52*, 8551-8556; (d) Nomura, D. K.; Dix, M. M.; Cravatt, B. F., Activity-based protein profiling for biochemical pathway discovery in cancer. *Nat. Rev. Cancer* **2010**, *10*, 630-638; (e) Cravatt, B. F.; Wright, A. T.; Kozarich, J. W., Activity-Based Protein Profiling: From Enzyme Chemistry to Proteomic Chemistry. *Annu. Rev. Biochem.* **2008**, *77*, 383-414.

(11) (a) Houtkooper, R. H.; Pirinen, E.; Auwerx, J., Sirtuins as regulators of metabolism and healthspan. *Nat. Rev. Mol. Cell Biol.* **2012**, *13*, 225-238; (b) Gallinari, P.; Di Marco, S.; Jones, P.; Pallaoro, M.; Steinkuhler, C., HDACs, histone deacetylation and gene transcription: from molecular biology to cancer therapeutics. *Cell Res.* **2007**, *17*, 195-211; (c) Wolffe, A. P., Histone Deacetylase--A Regulator of Transcription. *Science* **1996**, *272*, 371-372.

(12) (a) Li, L.; Shi, L.; Yang, S.; Yan, R.; Zhang, D.; Yang, J.; He, L.; Li, W.; Yi, X.; Sun, L.; Liang, J.; Cheng, Z.; Shi, L.; Shang, Y.; Yu, W., SIRT7 is a histone desuccinylase that functionally links to chromatin compaction and genome stability. *Nat. Commun.* **2016**, *7*, 12235; (b) Jiang, H.; Khan, S.; Wang, Y.; Charron, G.; He, B.; Sebastian, C.; Du, J.; Kim, R.; Ge, E.; Mostoslavsky, R.; Hang, H. C.; Hao, Q.; Lin, H., SIRT6 regulates TNF- α secretion through hydrolysis of long-chain fatty acyl lysine. *Nature* **2013**, *496*, 110-113; (c) Du, J.; Zhou, Y.; Su, X.; Yu, J. J.; Khan, S.; Jiang, H.; Kim, J.; Woo, J.; Kim, J. H.; Choi, B. H.; He, B.; Chen, W.; Zhang, S.; Cerione, R. A.; Auwerx, J.; Hao, Q.; Lin, H., Sirt5 Is a NAD-Dependent Protein Lysine Demalonylase and Desuccinylase. *Science* **2011**, *334*, 806-809.

(13) Huang, R.; Holbert, M. A.; Tarrant, M. K.; Curtet, S.; Colquhoun, D. R.; Dancy, B. M.; Dancy, B. C.; Hwang, Y.; Tang, Y.; Meeth, K.; Marmorstein, R.; Cole, R. N.; Khochbin, S.; Cole, P. A., Site-Specific

- Introduction of an Acetyl-Lysine Mimic into Peptides and Proteins by Cysteine Alkylation. *J. Am. Chem. Soc.* **2010**, *132*, 9986-9987.
- (14) Kölle, D.; Brosch, G.; Lechner, T.; Lusser, A.; Loidl, P. Biochemical methods for analysis of histone deacetylases. *Methods* **1998**, *15*, 323-331.
- (15) (a) Jamonnak, N.; Hirsch, B. M.; Pang, Y.; Zheng, W., Substrate specificity of SIRT1-catalyzed lysine N-epsilon-deacetylation reaction probed with the side chain modified N-epsilon-acetyl-lysine analogs. *Bioorg. Chem.* **2010**, *38*, 17-25; (b) Herman, D.; Jenssen, K.; Burnett, R.; Soragni, E.; Perlman, S. L.; Gottesfeld, J. M., Histone deacetylase inhibitors reverse gene silencing in Friedreich's ataxia. *Nat. Chem. Biol.* **2006**, *2*, 551-558.
- (16) (a) Liu, H.-W.; Chen, L.; Xu, C.; Li, Z.; Zhang, H.; Zhang, X.-B.; Tan, W., Recent progresses in small-molecule enzymatic fluorescent probes for cancer imaging. *Chem. Soc. Rev.* **2018**, *47*, 7140-7180; (b) Li, H.; Yao, Q.; Xu, F.; Xu, N.; Duan, R.; Long, S.; Fan, J.; Du, J.; Wang, J.; Peng, X., Imaging γ -Glutamyltranspeptidase for tumor identification and resection guidance via enzyme-triggered fluorescent probe. *Biomaterials* **2018**, *179*, 1-14; (c) Komatsu, T.; Urano, Y., Evaluation of Enzymatic Activities in Living Systems with Small-molecular Fluorescent Substrate Probes. *Anal. Sci.* **2015**, *31*, 257-265; (d) Minoshima, M.; Kikuchi, K., Chemical Tools for Probing Histone Deacetylase (HDAC) Activity. *Anal. Sci.* **2015**, *31*, 287-292.
- (17) Bao, X.; Wang, Y.; Li, X.; Li, X.-M.; Liu, Z.; Yang, T.; Wong, C. F.; Zhang, J.; Hao, Q.; Li, X. D., Identification of 'erasers' for lysine crotonylated histone marks using a chemical proteomics approach. *eLife* **2014**, *3*, e02999.
- (18) (a) Liu, G.; Park, S.-H.; Imbesi, M.; Nathan, W. J.; Zou, X.; Zhu, Y.; Jiang, H.; Parisiadou, L.; Gius, D., Loss of NAD-Dependent Protein Deacetylase Sirtuin-2 Alters Mitochondrial Protein Acetylation and Dysregulates Mitophagy. *Antioxid. Redox Signaling* **2016**, *26*, 849-863; (b) Lemos, V.; de Oliveira, R. M.; Naia, L.; Szegö, É.; Ramos, E.; Pinho, S.; Magro, F.; Cavadas, C.; Rego, A. C.; Costa, V.; Outeiro, T. F.; Gomes, P., The NAD⁺-dependent deacetylase SIRT2 attenuates oxidative stress and mitochondrial dysfunction and improves insulin sensitivity in hepatocytes. *Hum. Mol. Genet.* **2017**, *26*, 4105-4117.
- (19) Ozden, O.; Park, S.-H.; Wagner, B. A.; Yong Song, H.; Zhu, Y.; Vassilopoulos, A.; Jung, B.; Buettner, G. R.; Gius, D. SIRT3 deacetylates and increases pyruvate dehydrogenase activity in cancer cells. *Free Radical Biol. Med.* **2014**, *76*, 163-172.
- (20) Jing, H.; Hu, J.; He, B.; Negrón Abril, Y. L.; Stupinski, J.; Weiser, K.; Carbonaro, M.; Chiang, Y.-L.; Southard, T.; Giannakakou, P.; Weiss, R. S.; Lin, H., A SIRT2-Selective Inhibitor Promotes c-Myc Oncoprotein Degradation and Exhibits Broad Anticancer Activity. *Cancer Cell* **2016**, *29*, 297-310.
- (21) Al Shweiki, M. H. D. R.; Mönchgesang, S.; Majovsky, P.; Thieme, D.; Trutschel, D.; Hoehenwarter, W., Assessment of Label-Free Quantification in Discovery Proteomics and Impact of Technological Factors and Natural Variability of Protein Abundance. *J. Proteome Res.* **2017**, *16*, 1410-1424; (b) Gemperline, D. C.; Scalf, M.; Smith, L. M.; Vierstra, R. D., Morpheus Spectral Counter: A computational tool for label-free quantitative mass spectrometry using the Morpheus search engine. *Proteomics* **2016**, *16*, 920-924.
- (22) Zhou, Y.; Zhou, B.; Pache, L.; Chang, M.; Khodabakhshi, A. H.; Tanaseichuk, O.; Benner, C.; Chanda, S. K., Metascape provides a biologist-oriented resource for the analysis of systems-level datasets. *Nat. Commun.* **2019**, *10*, 1523.
- (23) Ashburner, M.; Ball, C. A.; Blake, J. A.; Botstein, D.; Butler, H.; Cherry, J. M.; Davis, A. P.; Dolinski, K.; Dwight, S. S.; Eppig, J. T.; Harris, M. A.; Hill, D. P.; Issel-Tarver, L.; Kasarskis, A.; Lewis, S.; Matese, J. C.; Richardson, J. E.; Ringwald, M.; Rubin, G. M.; Sherlock, G., Gene Ontology: tool for the unification of biology. *Nat. Genet.* **2000**, *25*, 25-29.
- (24) The Gene Ontology Consortium, Expansion of the Gene Ontology knowledgebase and resources. *Nucl. Acids Res.* **2017**, *45*, D331-D338.

Insert Table of Contents artwork here

